nature geoscience

SUPPLEMENTARY INFORMATION

DOI: 10.1038/NGEO2214

Satellite-based estimate of global aerosol-cloud radiative forcing by marine warm clouds

Y.-C. Chen, M. W. Christensen, G. L. Stephens, and J. H. Seinfeld

Supplementary Material

Supplementary Tables

Supplementary Figures

Supplementary References

Supplementary Material

Derivation of intrinsic and extrinsic AIE

The formal definition of TOA cloud radiative forcing can be written as: $C_{sw,lw} = F_{clr} - F_{obs}$, where F_{clr} is clear sky net radiative flux (i.e., $F_{clr} = F_{clr}^{\uparrow} - F_{clr}^{\downarrow}$ for atmospheric columns containing no clouds, where $F_{clr}^{\uparrow}$ is the TOA upward radiative flux, and $F_{clr}^{\downarrow}$ is the TOA downward radiative flux), and F_{obs} is the TOA net flux that is observed for all sky conditions (excluding ice clouds in this study). F_{obs} can be decomposed into $F_{obs} = (1 - c_f)F_{clr} + c_f F_{cld}$, where F_{cld} is the component of the radiative flux contributed by clouds. F_{cld} can be calculated using this equation. The equations for $C_{sw,lw}$ and F_{obs} can be combined to yield the following: $C_{sw,lw} = c_f(F_{clr} - F_{cld})$, for which the derivative of the shortwave (SW) component of the TOA cloud radiative forcing can be written as in Equation (1).

The longwave (LW) component of TOA cloud radiative forcing can be written similarly as:

$$\frac{dC_{lw}}{d\ln(AI)} = \left[\overline{c_m}\left(\frac{dF_{clr}}{d\ln(AI)} - \frac{dF_{cld}}{d\ln(AI)}\right) + \overline{(F_{clr} - F_{cld})}\frac{dc_f}{d\ln(AI)}\right]$$

Applying aerosol optical depth (AOD) and/or retrieved cloud droplet number concentration (N_d) as opposed to aerosol index (AI):

In this study, aerosol index (AI) is applied as the proxy for CCN to investigate aerosol-cloud interactions. Here we also consider AOD and N_d as alternative parameters to examine the extent to which similar responses would occur.

Assuming the liquid water content increases linearly with height in the cloud, N_d can be derived from the retrieved τ and R_e (e.g., George and Wood, 2010): $N_d = K\tau^{1/2}{R_e}^{-5/2}$, where $K = 1.125\times10^{-6}\mathrm{cm}^{-1/2}$, a weakly temperature/pressure-dependent thermodynamic constant. Applying the derived N_d as well as MODIS AOD to calculate the aerosol-cloud relationships as shown in Fig. 2, the cloud responses are very similar to those calculated using AI. The same trends are obtained for non-raining/raining clouds and different environmental scenario (not shown). This provides corroboration of the results obtained in the study.

Correlation between environmental conditions and aerosol index:

In Equation (1), $dA_{cld}/dln(AI)$ is calculated without considering the relationship between meteorology and aerosol index. To investigate the correlation between environmental conditions and AI, the following equation is considered:

$$\frac{dA_{cld}}{dln(AI)} = \frac{\partial A_{cld}}{\partial ln(AI)} + \frac{\partial A_{cld}}{\partial RH_{ft}}\frac{dRH_{ft}}{dln(AI)} + \frac{\partial A_{cld}}{\partial LTS}\frac{dLTS}{dln(AI)}$$

The partial derivatives are calculated using the cloudy pixels within each 4°×4° region between 60°S and 60°N from August 2006 to April 2011. Estimating the contributions of $\frac{\partial A_{cld}}{\partial RH_{ft}}\frac{dRH_{ft}}{dln(AI)}$ and $\frac{\partial A_{cld}}{\partial LTS}\frac{dLTS}{dln(AI)}$ to the total derivative, $\frac{dA_{cld}}{dln(AI)}$, these terms are ~4% and 2%, respectively, of the total magnitude. Thus, these two partial derivatives play a minor role in affecting the cloud albedo susceptibility. Consequently, we do not consider the correlation between meteorological condition and AI.

Intrinsic aerosol-cloud forcing:

The aerosol-cloud radiative forcing is calculated based on Equation (1) and (2) within each 4°×4° region between 60°S and 60°N from August 2006 to April 2011, as shown in Supplementary Fig. S2. The global mean aerosol-cloud radiative forcing is estimated by taking the geometric mean from the estimated forcing in each region. The same methods have been applied to estimate the forcing under different precipitation status and environmental conditions (Fig. 3).

Other than the absolute magnitude of aerosol-cloud radiative forcing in Fig. 3, the relative contribution of each individual regime is also reported in Supplementary Fig. S4. In Fig. S4, the relative magnitude of aerosol-cloud radiative forcing is weighted by the percentage of pixel numbers for each category. For example, non-raining and raining clouds account for 82.9% and 17.1% of the data set, respectively; the relative magnitude is the absolute forcing (shown in Fig. 3) times the corresponding percentage of data (i.e., $-0.46 \times 82.9\%$ and $-0.67 \times 17.1\%$ for non-raining and raining clouds, respectively). Without considering the percentage of pixel numbers, the raining clouds reveal stronger forcing as compared to non-raining clouds, showing the cloud albedo sensitivity to AI is higher for raining clouds. Yet due to the low occurrence of precipitation, the relative contribution of raining clouds becomes lower than non-raining clouds.

Considering different hemisphere, the Northern and Southern hemisphere covers 32.5% and 67.5% of the data set, respectively. By weighting the data percentage to the absolute magnitude, the Southern hemisphere has larger relative contribution in aerosol-cloud radiative forcing than the Northern hemisphere.

The intrinsic aerosol-cloud radiative forcing reflects the R_e and LWP changes in response to aerosol. LWP is not held constant in the estimation of intrinsic AIE, and thus this definition differs from the so-called Twomey effect. Lebsock et al. (2008) also estimated the first aerosol indirect effect for oceanic warm clouds using A-Train satellite observations. The magnitude obtained here (-0.49 $\pm$0.33 Wm^{-2}) is close to that reported by Lebsock et al. (2008) (-0.42 Wm^{-2}).

Previous studies have also reported the aerosol indirect forcing over the ocean (not limited to warm clouds). These include: -0.8$\pm$0.5 Wm^{-2} under all-sky condition over ocean (Bellouin et al., 2013); -0.93$\pm$0.44 and -0.82$\pm$0.52 Wm^{-2} for ocean cloudy-sky condition from model and scaled model estimates, respectively (Quaas et al., 2009); -0.2$\pm$0.1 Wm^{-2} over ocean (satellite-based estimation; Quaas et al., 2008). These values are listed as references for related studies using different data and methods.

Uncertainty in the magnitude of extrinsic aerosol-cloud forcing:

The extrinsic aerosol-cloud forcing may be sensitive to the resolution of the cloud fraction applied. When applying MODIS 1° cloud fraction as opposed to CERES 20 km cloud fraction to estimate extrinsic AIE, the magnitude is about three times larger. This may be related to the scale problem associated with coarser resolution (McComiskey and Feingold, 2012). More detailed analysis is needed to study this potential issue. The error estimation we provided in the study is that based on linear regression, and does not include other sources of uncertainties. We also compared the results at different resolutions of AI (i.e., AI in 20 km and 1° resolution from MODIS). We find that the

aerosol-cloud forcing is insensitive to the spatial resolution of AI, indicating that the spatial distribution of aerosol is relatively uniform throughout the region.

Supplementary Tables

Supplementary Table S1. Multiple sensors, parameters, and their corresponding spatial resolutions applied in the study.

Sensor	Parameter	Spatial Resolution
CloudSat	Precipitation flag	1.4 × 2.5 km
MODIS	3.7 μm R_e, τ	1 × 1 km
	Cloud top pressure/temperature	5 × 5 km
	Cloud fraction, AOD, aerosol index	1° × 1°
CALIPSO	Cloud top height, cloud layer flag, aerosol top/base heights	5 × 5 km (vertical 30 m)
CERES	Albedo, cloud fraction, cloud phase	20 × 20 km
AMSR-E	Cloud LWP	13 km
ECMWF	Pressure, temperature, humidity	2.5° × 2.5°
MACC	Aerosol species, AOD	120 × 120 km

Supplementary Table S2. Criteria and data screening for the selection of single layer low-level marine warm phase clouds.

Criteria	Percent
Warm ocean clouds (MODIS cloud top P and T) + valid MODIS cloud parameter and CERES radiation	100% (~26 million)
Above + CERES cloud phase	75%
Above + single cloud layer (CALIPSO)	53%
Above + valid CERES cloud albedo and solar angle+ valid MODIS aerosol index (AI)	28% (~7.3 million data)

Supplementary Figures

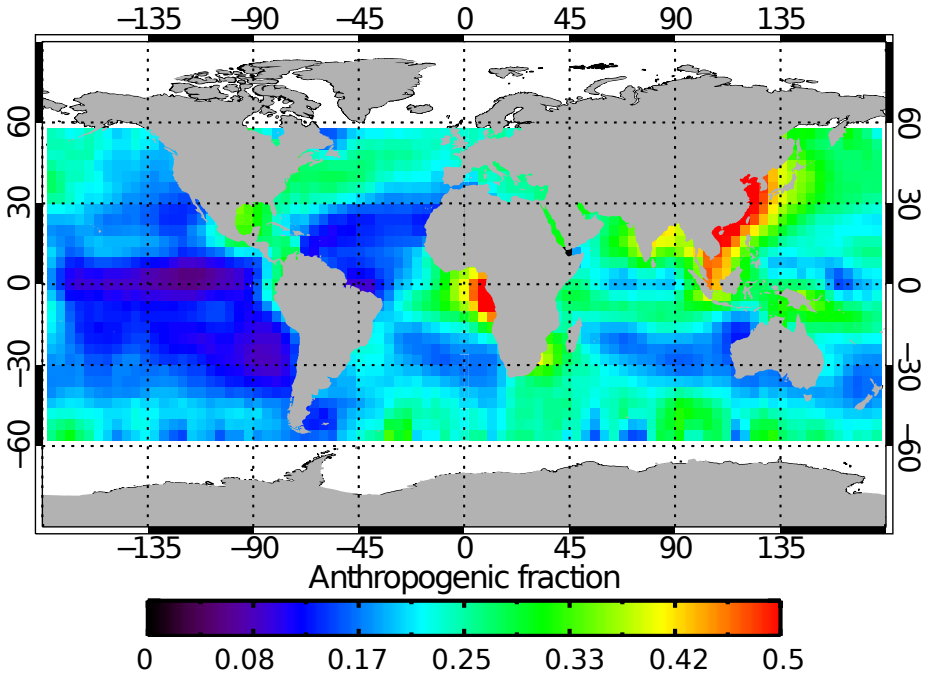

Supplementary Figure S1. Global distribution of aerosol anthropogenic fraction based on MACC product and algorithms in Bellouin et al. (2013). Each colored pixel represents the mean value for the selected pixels within each 4°×4° region between 60°S and 60°N from August 2006 to April 2011.

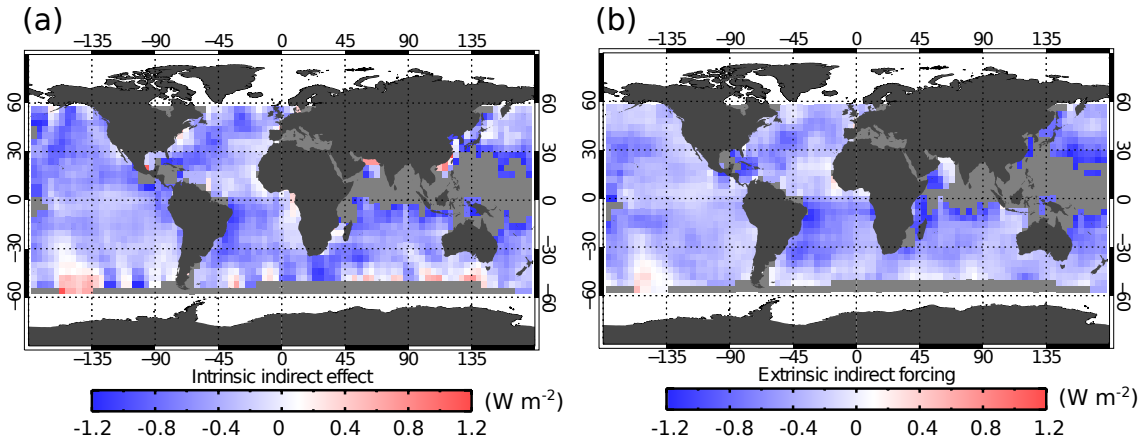

Supplementary Figure S2. Global distribution of (a) intrinsic aerosol indirect forcing and (b) extrinsic aerosol indirect forcing, following Equation (1) and (2). Each colored pixel represents the value within a 4°×4° region between 60°S and 60°N from August 2006 to April 2011. The gray regions are the ones with data points less than 1000 and thus not included.

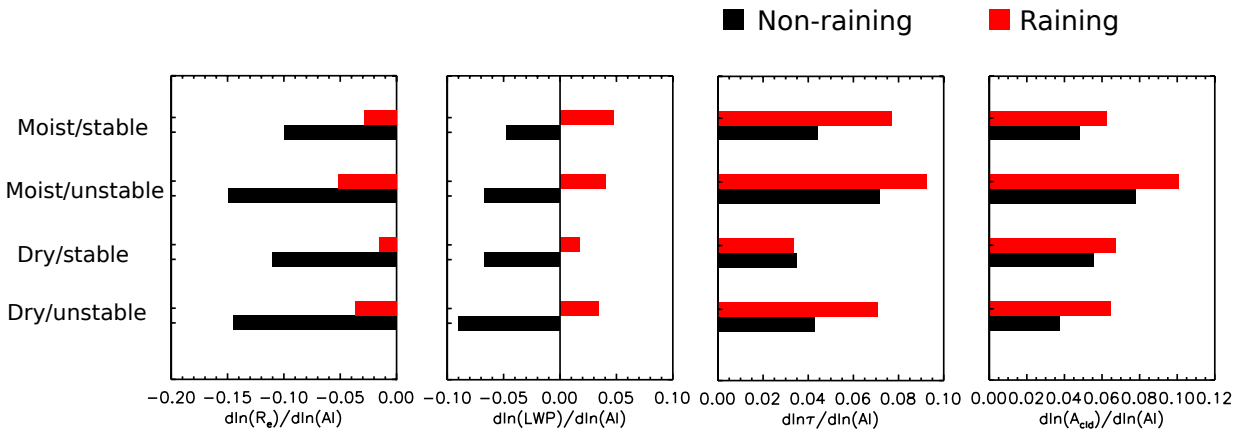

Supplementary Figure S3. The same as Fig. 2, except the natural logarithm of cloud properties are applied to show the inherent sensitivity between cloud properties and AI.

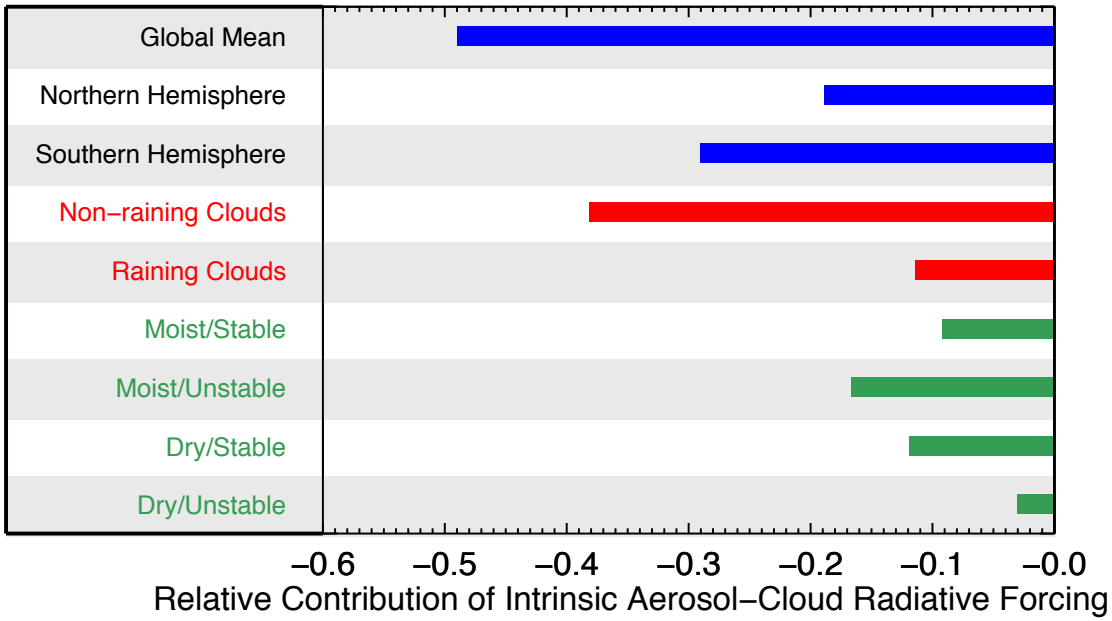

Supplementary Figure S4. The same as Fig. 3, except the magnitude of aerosol-cloud radiative forcing (W m^{-2}) for each regime is weighted by the percentage of pixel numbers under each category (see Supplementary Material).

Supplementary References

George, R. C. & Wood, R. Subseasonal variability of low cloud radiative properties over the southeast Pacific Ocean, *Atmos. Chem. Phys.*, **10**, 4047–4063 (2010).

Quaas, J. et al. Aerosol indirect effects — General circulation model intercomparison and evaluation with satellite data. *Atmos. Chem. Phys.*, **9**, 8697-8717 (2009).

Quaas, J., Boucher, O., Bellouin, N. & Kinne, S. Satellite-based estimate of the direct and indirect aerosol climate forcing, *J. Geophys. Res.,* **113**, D05204 (2008).

McComiskey, A. & Feingold, G. The scale problem in quantifying aerosol indirect effects, *Atmos. Chem. Phys.,* **12**, 1031-1049 (2012).